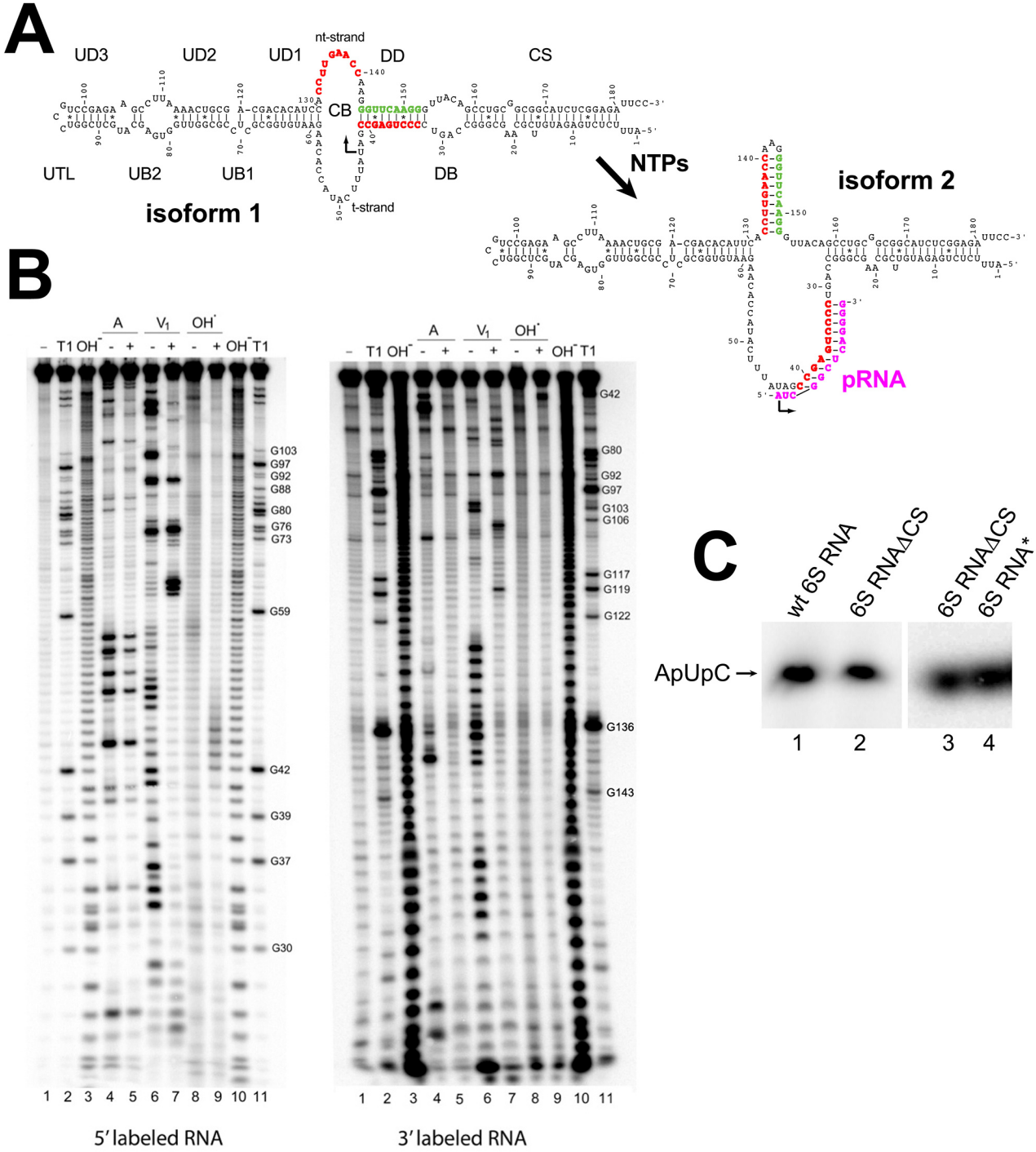

Chen et al., Figure S1

Figure S1. 6S RNA structural transition and footprinting. Related to Figures 1 and 2.

(**A**) The pRNA-induced structural transition of 6S RNA (Beckmann et al., 2012; Panchapakesan and Unrau, 2012). (*top left*) Secondary structure of wild-type 6S RNA isoform 1 (*top left*) and isoform 2 (*bottom right*). Isoform 2 is stabilized by the RNAP-mediated synthesis of pRNA (magenta).

(**B**) RNAse footprinting gels: T1 shows cleavage by RNase T1 specific for G-residues, their positions are indicated on the right side of gels, A and V_1 – cleavage by RNAse A (cleaves 3' of U and C residues) and V_1 (cleaves base-paired nucleotides), respectively. OH* represents hydroxyl radical cleavage, OH^- - Alkaline Hydrolysis under single hit conditions, resulting in an RNA 'ladder' with single nucleotide resolution.

(*left*) 5'-labeled RNA. '-' and '+' indicates absence or presence of $E\sigma^{70}$, respectively.

(*right*) 3'-labeled RNA.

(**C**) Relative abortive transcription activity of wild-type 6S RNA (lane 1) and 6S RNA with the CS truncated (6S RNAΔCS, lane 2), and 6S RNAΔCS (lane 3) and 6S RNA* (lane 4).

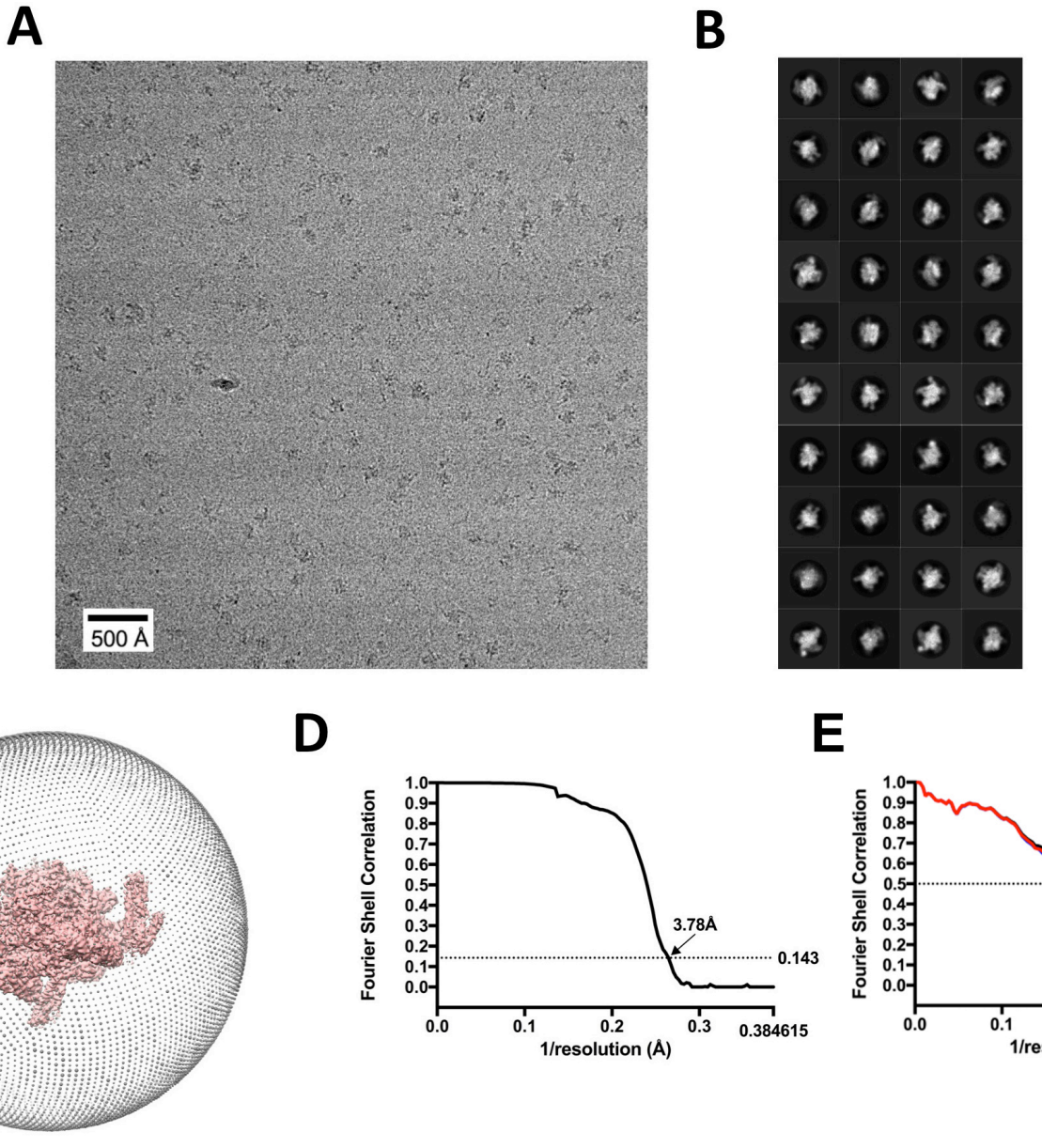

Chen et al., Figure S2

Figure S2. CryoEM of the 6S RNA/Eσ^{70} complex. Related to Figure 1.

(**A**) Representative micrograph of the 6S RNA/Eσ^{70} complex in vitreous ice.

(**B**) The forty highest populated classes from 2D classification.

(**C**) Angular distribution for 6S RNA/Eσ^{70} particle projections.

(**D**) Gold-standard FSC of the 6S RNA/Eσ^{70} complex. The gold-standard FSC was calculated by comparing the two independently determined half-maps from RELION. The dotted line represents the 0.143 FSC cutoff, which indicates a nominal resolution of 3.78 Å.

(**E**) FSC calculated between the refined structure and the half map used for refinement (work), the other half map (free), and the full map.

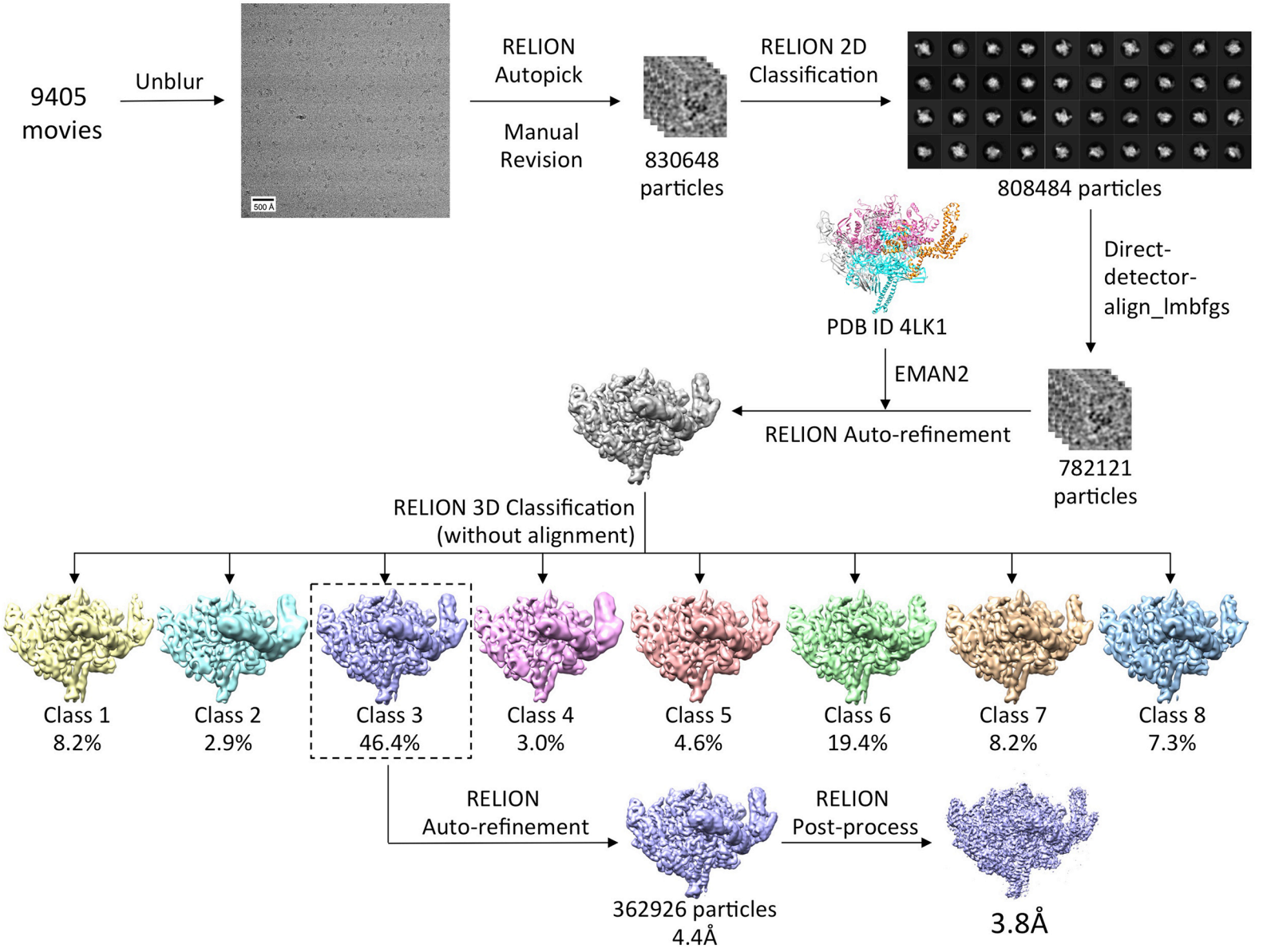

Chen et al., Figure S3

Figure S3. Data processing pipeline for the cryoEM data. Related to Figure 1.

Flowchart showing the image processing pipeline for the cryoEM data of *Eco* 6S RNA*/ΔαCTD-E-Δ1.1σ^{70} starting with 9,405 dose-fractionated movies collected on a 300 keV Titan Krios (FEI) equipped with a K2 Summit direct electron detector (Gatan). Movie frames were aligned and summed using Unblur (Grant and Grigorieff, 2015). Particles were autopicked and manually revised from these summed images and then sorted by 2D classification in RELION (Scheres, 2012) for subsequent particle polishing using direct-detector-align_lmbfgs software (Rubinstein and Brubaker, 2015). After polishing, the dataset contained 782,121 aligned particles. These particles were auto-refined in RELION using a model of *Eco* Eσ^{70} (PDB ID 4LK1) (Bae et al., 2013) that was low-pass filtered to 60 Å resolution using EMAN2 (Tang et al., 2007) as an initial 3D template. 3D classification into eight classes was performed on the particles using the refined model and alignment angles. No obvious conformational differences were observed between the 3D classes. Class 3, containing 362,926 particles, was the most populated class with a 3.8 Å resolution after auto-refinement and post-processing in RELION.

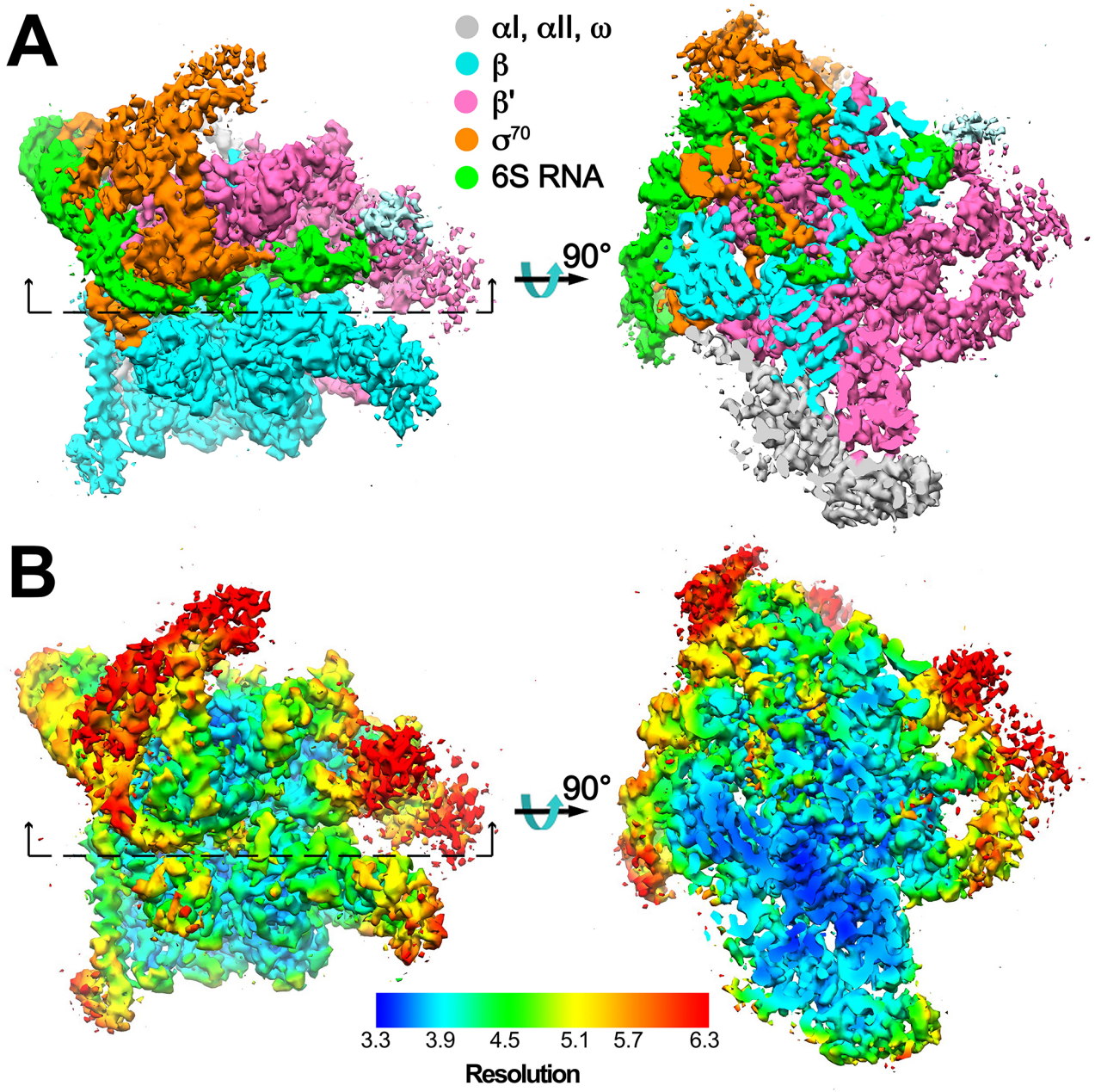

Chen et al., Figure S4

Figure S4. Overall cryo-EM map and local resolution of 6S RNA/Eσ^{70}. Related to Figure 1.

(**A**) The 3.8-Å resolution cryoEM density map of the 6S RNA/Eσ^{70} complex colored according to the legend at the top. The view on the right shows a cross section at the position indicated in the left panel.

(**B**) Same views of the cryoEM density map as in **A**, but colored by local resolution (Cardone et al., 2013).

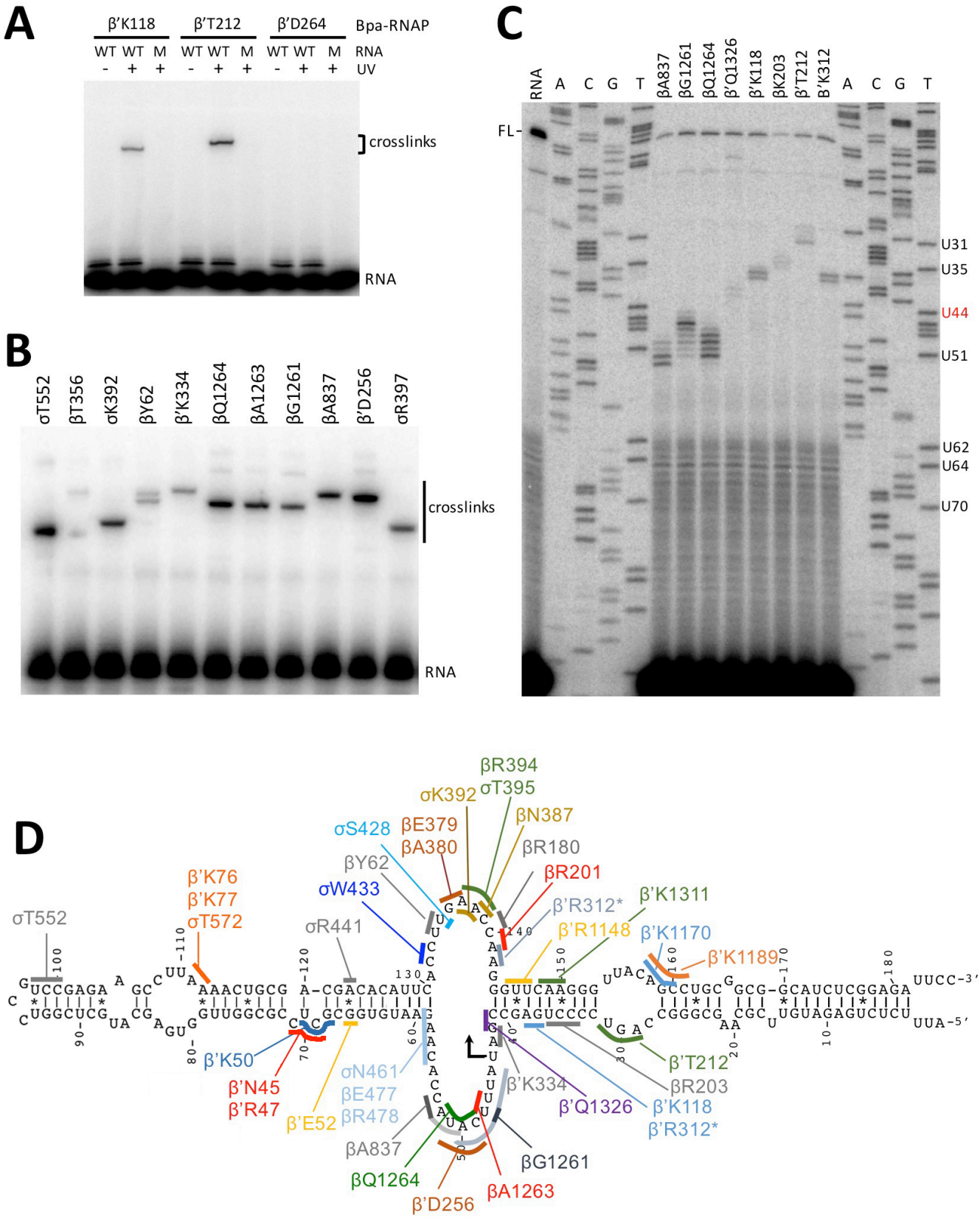

Chen et al., Figure S5

Figure S5. BPA-dependent crossliking to 6S RNA and crosslink mapping. Related to Figure 2.

(**A**) 6S RNA crosslinking to BPA-substituted RNAP is dependent on UV irradiation and position of BPA substitutions. ^{32}P-labelled RNA [WT, wild-type 6S RNA; M, 6S(M5) RNA] (2 nM) was incubated with BPA-substituted Eσ^{70} (position of BPA substitutions indicated at top)(~100 nM), exposed to 365-nm light (+UV) or kept in the dark (-UV), and separated on NuPage protein gels. Uncrosslinked RNA is observed near the bottom of the gel (RNA) and crosslinked RNA migrates more slowly in the gel (crosslinked RNA). 6S(M5) RNA is an inactive mutant with a severely reduced central bubble (Trotochaud and Wassarman, 2005). BPA substitutions at β'K118 and β'T212 crosslink to 6S RNA in a UV-dependent manner, but not the inactive M5 mutant. BPA substitution at β'D264 does not crosslink to RNA.

(**B**) An example of crosslinking results with different BPA-substituted RNAPs on ^{32}P-labeled 6S RNA.

(**C**) An example of primer extension mapping of BPA crosslinking positions in 6S RNA. Unlabelled 6S RNA was incubated with BPA-substituted Eσ^{70} (position of BPA substitutions indicated at top)(~100 nM), exposed to 365-nm light, followed by Ni-NTA enrichment of crosslinked RNAs (see Methods). Enriched RNAs were used as template for primer extension reactions using ^{32}P-labeled KW1469 primer (complementary to nucleotides 88-111 in 6S RNA) and separated on a 10% denaturing polyacrylamide gel run with a salt gradient. Sequencing reactions (A, C, G, T) were generated with the same labeled primer for reference. The first lane (RNA) is primer extension from uncrosslinked RNA for reference.

(**D**) Mapped BPA-crosslinking positions from BPA-substituted RNAPs are indicated on the secondary structure of 6S RNA. Some positions crosslink to multiple nearby nucleotides, as represented by the lines covering RNA nucleotides.

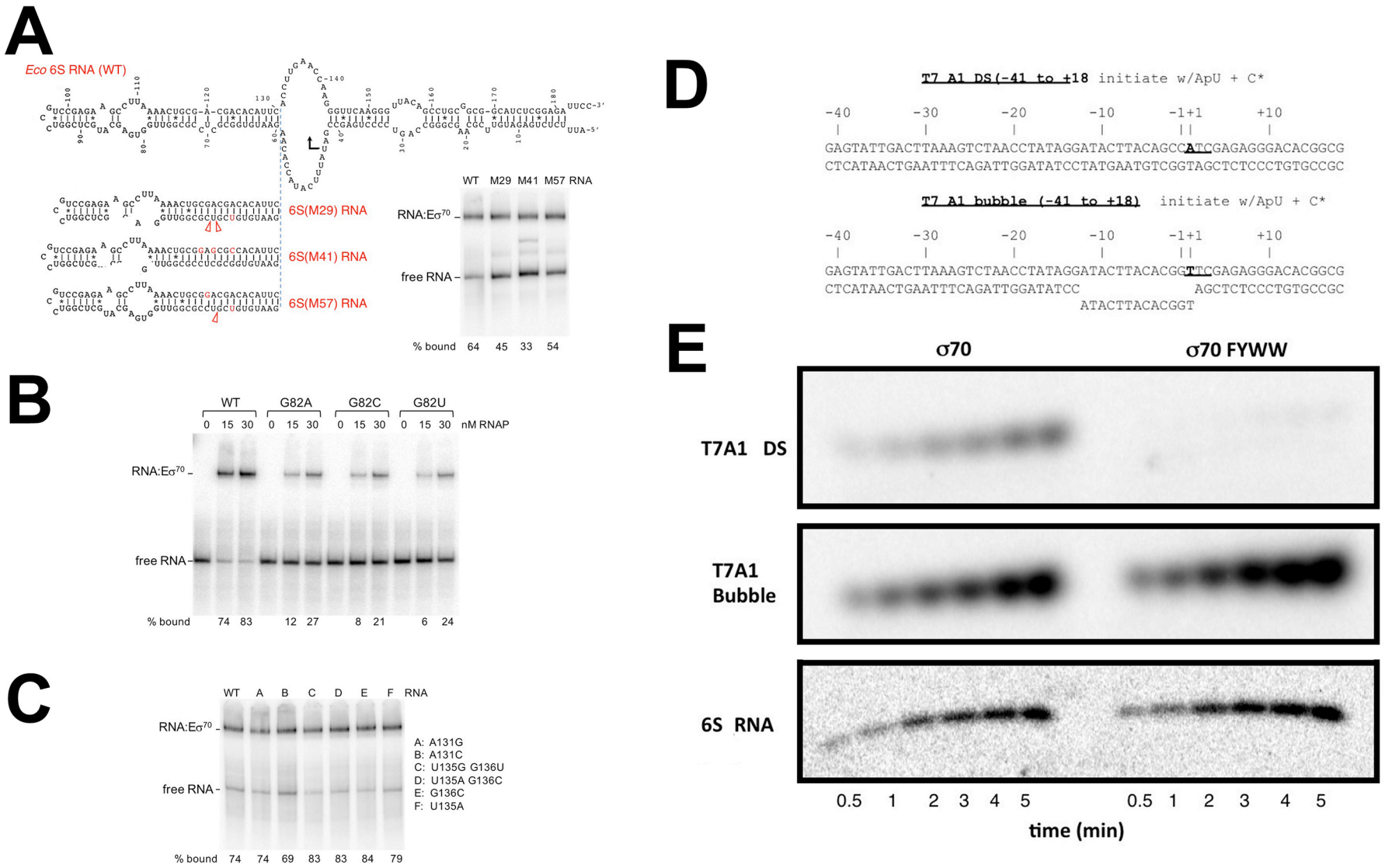

Chen et al., Figure S6

Figure S6. Effects of 6S RNA modifications on Eσ^{70} binding, and 6S RNA is pre-melted and does not require the σ^{70} W-dyad for transcription bubble stabilization. Related to Figures 5 and 6.

(**A**) Illustration of the changes made to remove UB1. Different changes were made that all resulted in basepairing through the UB1 region, but with different effects on the length of the upstream stem. Note, residues changed from wild type or inserted are in red; the red triangles indicate the locations of deleted nucleotides. (*lower right*) A native gel electrophoresis binding assay illustrates the decrease in 6S RNA binding when UB1 is absent.

(**B, C**) Native gel electrophoresis binding assays illustrating the strong effect of 6S RNA G82 substitutions on 6S RNA binding (**B**), the absence of altered binding for 6S RNA substitutions at A131, U135, or G136 (**C**).

(**D**) Sequences of the duplex T7 A1 promoter (*top*) and the T7 A1 bubble promoter (*bottom*).

(**E**) Abortive transcription activity (ApUpC synthesis) of Eσ^{70} (left panel) and melting-deficient Eσ^{70}_{FYWW} (Tomsic et al., 2001) on duplex T7 A1 (T7A1 DS, top row), T7 A1 bubble (middle row), and 6S RNA (bottom row).

A

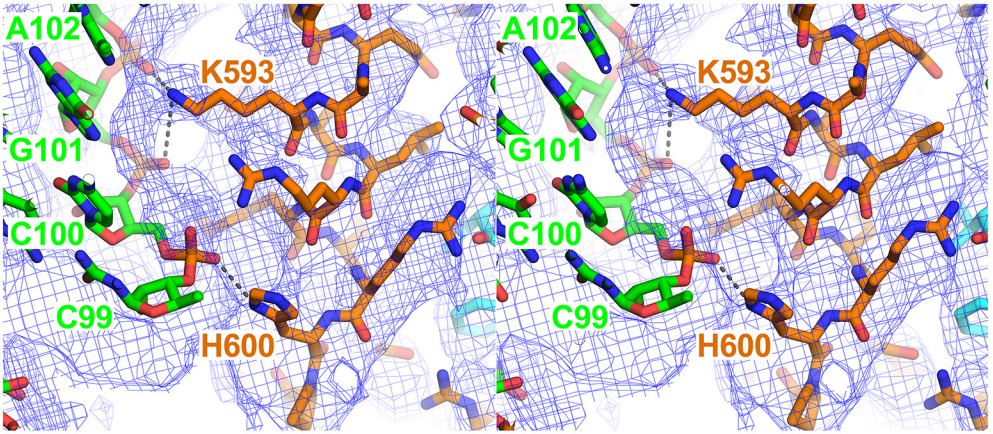

B

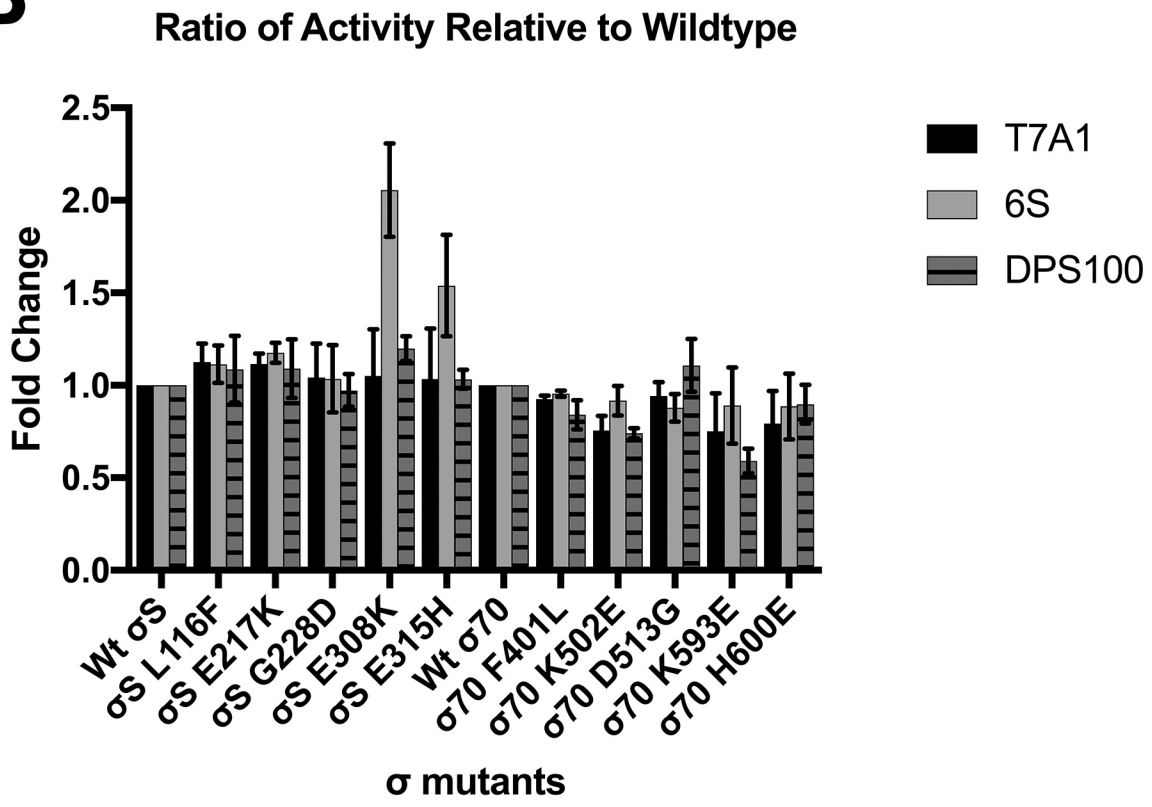

Chen et al., Figure S7

Figure S7. Interactions between σ^{70} K593 and H600 with 6S RNA, and normalized abortive transcription activity of σ mutants. Related to Figure 7.

(**A**) Stereo view of the 6S RNA/Eσ^{70} cryoEM density map (blue mesh) showing the interaction of σ^{70} K593 and H600 with the 6S RNA phosphate backbone.

(**B**) Histogram showing the normalized abortive transcription initiation activity for the indicated σ's (bottom) on the indicated templates (σ^{70}-specific promoter T7A1; σ^{70}-specific 6S RNA; σ^{S}-specific promoter DPS (Grainger et al., 2008)). The σ^{S}-holoenzyme activities are shown normalized with respect to wild-type σ^{S}, while the σ^{70}-holoenzymes are shown normalized to wild-type σ^{70}. The histograms represent the average of at least three measurements, the error bars denote S.E.M.s.

Table S1. Model statistics from Molprobity (Chen et al., 2010)**.**
Related to Figure 1.

		6S RNA/Eσ^{70}
Overall	Resolution[a]	3.78 Å
	Molprobity score	1.83
	Clashscore (all atoms)	6.56
	RMS deviations bonds (Å)	0.007
	RMS deviations angles (°)	1.027
Protein (3,132 residues)	Rotamer outliers	0.54%
	Ramachandran favored	92.57%
	Ramachandran outliers	0.08%
RNA[b] (112 nucleotides)	Probably wrong sugar puckers	0
	Bad backbone conformations	3 (2.68%)

[a] Gold-standard FSC 0.143 cutoff criteria (Figure S2D) (Rosenthal and Henderson, 2003).

[b] ref. (Richardson et al., 2008)

Table S2. Minor and major groove widths and axial base pair rise for 6S RNA[a]. Related to Figure 4.

6S RNA element[b]	Strand I	step	Strand II	Minor groove P-P (Å)[c]	Major groove P-P (Å)[c]	Rise (Å)	Twist (°)	Pitch (Å)
DD*	32-33	CG/CG	152-153			3.6	28	41
	33-34	GG/CC	151-152			2.9	32	
	34-35	GC/AC	150-151	11.5	10.4	2.8	33	
	35-36	CA/UA	149-150	11.2	11.9	4.4	29	
	36-37	AC/GU	148-149	10.7	13.2	3.2	31	
	37-38	CA/UG	147-148	10.5	15.2	3.4	24	
	38-39	AU/GU	146-147	10.6	13.8	3.1	39	
	39-40	UG/CG	145-146			3.7	18	
	40-41	GC/GC	144-145			3.3	31	
UD1	59-60	GA/UC	129-130			2.9	32	35
	60-61	AA/UU	128-129	10.9	14.9	3.2	30	
	61-62	AU/AU	127-128	10.7	12.9	3.2	28	
	62-63	UG/CA	126-127	10.7	12.7	3.4	27	
	63-64	GU/AC	125-126	10.8	12	3.2	32	
	64-65	UG/CA	124-125	10.9	11.1	3.2	31	
	65-66	GG/AC	123-124	10.6	10.6	3.1	30	
	66-67	GC/GA	122-123	9.3	9.9	3.2	31	
	67-68	CG/CG	121-122	9.9	8.8	2.9	33	
UD2	72-73	CG/CG	118-119	10.8	9.2	4.4	30	33
	73-74	GC/GC	117-118	10.7	11.2	3.1	35	
	74-75	CG/UG	116-117	11.0	12.1	3.3	26	
	75-76	GG/CU	115-116	11.5	11	2.9	33	
	76-77	GU/AC	114-115	11.8	10.3	3.1	32	
	77-78	UU/AA	113-114			3.1	29	
	78-79	UG/AA	112-113			1.4	49	
UD3	88-89	GC/GA	103-104	13.3	15	3.2	39	31
	89-90	CU/AG	102-103	12.1	10.8	3.0	25	
	90-91	UC/GA	101-102	12.1	11.5	2.9	30	
	91-92	CG/CG	100-101	11.9	10.9	2.6	34	
	92-93	GG/CC	99-100			3.0	37	
	93-94	GU/UC	98-99			2.9	39	
				Canonical A-form nucleic acid[d]	Canonical B-form nucleic acid[d]	6S RNA (average)		
			Rise (Å)	2.6	3.4	3.2 ± 0.5		
			Twist (°)	33	36	32 ± 6		
			Pitch (Å)	28	34	35 ± 4		

[a]Parameters calculated using 3DNA (Lu and Olson, 2008).

[b]See Figure 1A.

[c]Direct P-P distances (with van der Waals radii of phosphate groups, 5.8 Å, subtracted.

[d]ref. (Egli and Saenger, 2013).

Table S3. Sugar puckers for 6S RNA[a]. Related to Figure 4.

	Strand I			Strand II	
6S RNA element	nucleotide	Sugar pucker		nucleotide	Sugar pucker
DD*	32C	C3'-endo		153G	C3'-endo
	33G	C3'-endo		152C	C3'-endo
	34G	C3'-endo		151C	C3'-endo
	35C	C3'-endo		150A	C3'-endo
	36A	C3'-endo		149U	C3'-endo
	37C	C3'-endo		148G	C3'-endo
	38A	C3'-endo		147U	C3'-endo
	39U	C3'-endo		146G	C3'-endo
	40G	C3'-endo		145C	C3'-endo
	41C	C3'-endo		144G	C3'-endo
UD1	59G	C3'-endo		130C	C3'-endo
	60A	C3'-endo		129U	C3'-endo
	61A	C3'-endo		128U	C3'-endo
	62U	C3'-endo		127A	C3'-endo
	63G	C3'-endo		126C	C3'-endo
	64U	C3'-endo		125A	C3'-endo
	65G	C3'-endo		124C	C3'-endo
	66G	C3'-endo		123A	C3'-endo
	67C	C3'-endo		122G	C3'-endo
	68G	C3'-endo		121C	C3'-endo
UD2	72C	C3'-endo		118G	C3'-endo
	73G	C1'-endo		117C	C3'-endo
	74C	C3'-endo		116G	C3'-endo
	75G	C3'-endo		115U	C3'-endo
	76G	C3'-endo		114C	C3'-endo
	77U	C3'-endo		113A	C3'-endo
	78U	C3'-endo		112A	C3'-endo
	79G	C3'-endo		111A	C2'-endo
UD3	88G	C3'-endo		104A	C3'-endo
	89C	C3'-endo		103G	C3'-endo
	90U	C3'-endo		102A	C3'-endo
	91C	C3'-endo		101G	C3'-endo
	92G	C3'-endo		100C	C2'-exo
	93G	C3'-endo		99C	C3'-endo
	94U	C3'-endo		98U	C3'-endo

[a]Calculated using 3DNA (Lu and Olson, 2008).

Table S4. Intrastrand P—P virtual bond distances[a]. Related to Figure 4.

6S RNA element[b]	Strand I	step	Intrastrand P—P distance (Å)		Strand II	step	Instrastrand P—P distance (Å)
DD*	32-33	CG	6.0		152-153	CG	5.8
	33-34	GG	6.5		151-152	CC	5.8
	34-35	GC	5.7		150-151	AC	5.9
	35-36	CA	5.6		149-150	UA	5.9
	36-37	AC	5.7		148-149	GU	6.4
	37-38	CA	6.0		147-148	UG	5.6
	38-39	AU	5.9		146-147	GU	6.6
	39-40	UG	5.8		145-146	CG	5.8
	40-41	GC	5.6		144-145	GC	5.4
UD1	59-60	GA	6.3		129-130	UC	5.6
	60-61	AA	7.0		128-129	UU	6.0
	61-62	AU	5.5		127-128	AU	5.8
	62-63	UG	5.9		126-127	CA	5.8
	63-64	GU	5.6		125-126	AC	5.7
	64-65	UG	5.9		124-125	CA	5.8
	65-66	GG	5.8		123-124	AC	6.3
	66-67	GC	5.3		122-123	GA	5.7
	67-68	CG	6.5		121-122	CG	6.2
UD2	72-73	CG	5.7		118-119	CG	5.7
	73-74	GC	6.8		117-118	GC	6.6
	74-75	CG	5.8		116-117	UG	6.1
	75-76	GG	5.7		115-116	CU	5.6
	76-77	GU	6.0		114-115	AC	5.8
	77-78	UU	5.6		113-114	AA	4.9
	78-79	UG	6.2		112-113	AA	8.5
UD3	88-89	GC	5.1		103-104	GA	6.4
	89-90	CU	5.2		102-103	AG	6.2
	90-91	UC	5.3		101-102	GA	5.7
	91-92	CG	5.8		100-101	CG	6.4
	92-93	GG	5.8		99-100	CC	7.0
	93-94	GU	5.3		98-99	UC	6.8

	Canonical A-form nucleic acid[d]	Canonical B-form nucleic acid[d]	6S RNA (average)
Intrastrand P—P distance (Å)[c]	5.9	7.0	6.0 ± 0.8

[a]Parameters calculated using 3DNA (Lu and Olson, 2008).

[b]See Figure 1A.

[c] ref. (Egli and Saenger, 2013).